Materials Science in Semiconductor Processing 120 (2020) 105271

Contents lists available at ScienceDirect

Materials Science in Semiconductor Processing

journal homepage: http://www.elsevier.com/locate/mssp

Silicon damage control through the use of aromatic hydrocarbon ion implantation

KyungWon Lee [a,b], Michael Saied Ameen [b], Mark Alan Harris [b], Dwight Dongwan Roh [b], Ronald Norman Reece [b], DaeHo Yoon [a,*]

[a] Sungkyunkwan University, 2066, Seobu-ro, Jangan-gu, Suwon-si, Gyeonggi-do, 16419, Republic of Korea
[b] Axcelis Technologies, Inc, 108 Cherry Hill Dr, Beverly, MA, 01915, USA

ARTICLE INFO

Keywords:
Ion implantation
Molecular carbon
Carbon implant
Aromatic hydrocarbon
Amorphous layer

ABSTRACT

The continuous shrinking of transistor devices calls for precise doping profile control. Generally, monomer carbon (C+) is implanted at doses too low to adequately form an amorphous layer in silicon. Previous experiments used a molecular carbon species combined with dedicated vaporizer-based hardware, but this experiment was carried out using a commercial implanter and source with a liquid precursor material. The use of higher mass molecular carbon ions, such as $C_7H_7^+$, impart significantly more damage to the silicon than the monomer, and can easily result in a well-defined amorphous layer. There are many species of molecular carbon that can be implanted, but in order to utilize a hot cathode plasma (HCP) ion source some additional criteria must be met. The source feed material should fragment with high-yield of molecular carbon (C_x^+, x = 2–8) ions, which could then be extracted at beam currents sufficient to meet production needs using standard ion implant techniques. In this work, we surveyed several candidates for forming the molecular carbon species that could meet the requirements outlined above, reported the performance in plasma formation, and investigated materials properties of the Si after implantation.

1. Introduction

As the device node becomes smaller, precise doping profile control is required in transistors [1]. Boron is widely used as a P-type dopant [2], however it exhibits transient enhanced diffusion (TED) effect during thermal processing for activation, which makes profile control difficult in such small dimensions. Carbon co-implantation is used to suppress TED effect. Research has established that junction control can be enabled by using pre-amorphization implants (PAI) along with carbon co-implantation to suppress TED of implanted boron dopants. When activating boron dopants with annealing, the boron can experience higher rates of diffusion due to residual damage in the silicon. The carbon acts to capture this damage and thereby enables a more controllable profile of the boron. The amorphous layer formed by PAI improves the activation of the boron, so an ideal scenario would be formation of the amorphous layer with the carbon implant, allowing both diffusion control and high activation of the boron dopants [3–5]. TED is a known artifact related to interaction of Si-damage with boron diffusion during annealing, which occurs through interstitial transport in silicon. Carbon acts to tie up the interstitial vacancies thereby reducing the TED effect.

Prior to boron implantation, a PAI is also required to generate shallow junction profiles [6–8]. The amorphization layer thickness is a function of implant damage, and is correlated with dose, energy, mass, temperature, and instantaneous dose rate during the implant [9–11]. The dose and energy are typically fixed based on device schematic and characteristics [12]. We may also consider implant mass which has flexibility depending on the source material. Si damage is directly dependent on the mass of the ion, and using a molecular species will increase the damage for a given energy and dose. There are many molecular carbon materials that have proper vapor pressures suitable to gas delivery to an ion source [13]. There were several experiments using molecular carbon in specialized, dedicated, vaporizer hardware previously [14,15]. Ideally it is desirable to use a gas precursor for the HCP ion source [16]. Our goal is to generate the amorphous layer by using single molecular carbon process with higher mass implantation instead of a 2-step implant with monomer carbon and PAI process.

* Corresponding author.
E-mail address: dhyoon@skku.edu (D. Yoon).

https://doi.org/10.1016/j.mssp.2020.105271
Received 17 January 2020; Received in revised form 31 May 2020; Accepted 13 June 2020
Available online 11 July 2020

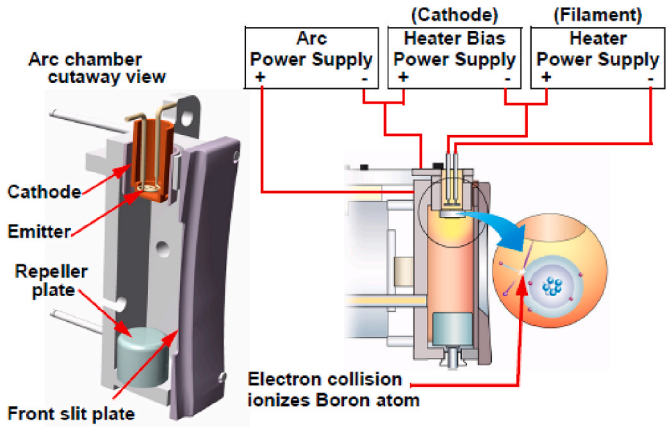

Fig. 1. Hot Cathode Plasma (HCP) diagram.

2. Experimental

HCP is a well-established type of ion source used for mass production. In this experiment, we used the Axcelis Enhanced Lifetime Source (ELS™) shown in Fig. 1. To generate plasma, gas-phase source material is required in an HCP arc chamber [17]. This source operates in the following manner with low-E−5 Pa chamber pressure, 25 V of arc voltage, ~0.8 mA of arc current: a cathode, typically constructed from tungsten, is heated by a filament (indirect heating) to create thermionic electrons. These electrons are accelerated into the arc chamber which is 100 mm × 50 mm X 50 mm that contains the gas to be ionized. A plasma is generated consisting of ionized fragments of molecules, ionized atoms, and neutrals. The ionic components are extracted through the arc slit and extraction electrode assembly, then injected into the implanter beamline. Subsequent beamline elements will resolve the correct atomic mass unit (AMU), focus the beam, and scan the beam over the wafer. This type of source is proven in mass production for ion implantation, and has been well characterized previously [17].

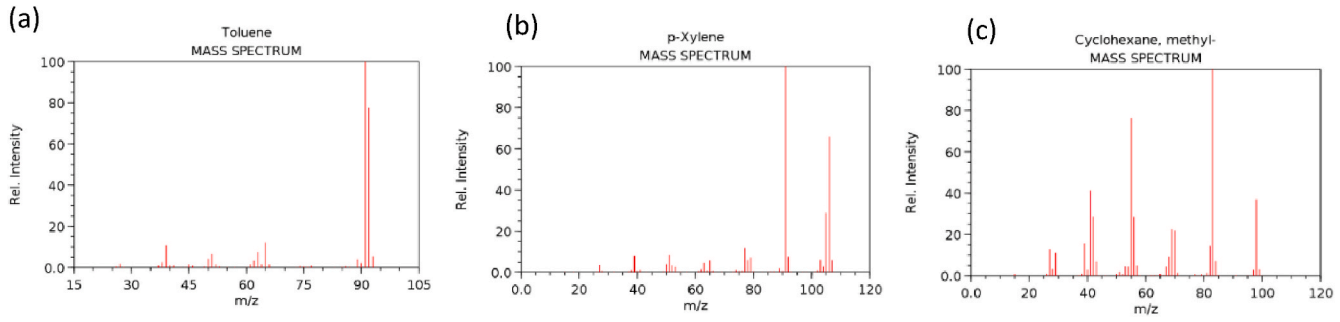

Fig. 2. Molecular carbon mass spectrum (electron ionization), (a) Toluene (C_7H_8), (b) p-Xylene (C_8H_{10}), (c) Methyl cyclohexane (C_7H_{14}). NIST chemistry WebBook (https://webbook.nist.gov/chemistry) [18].

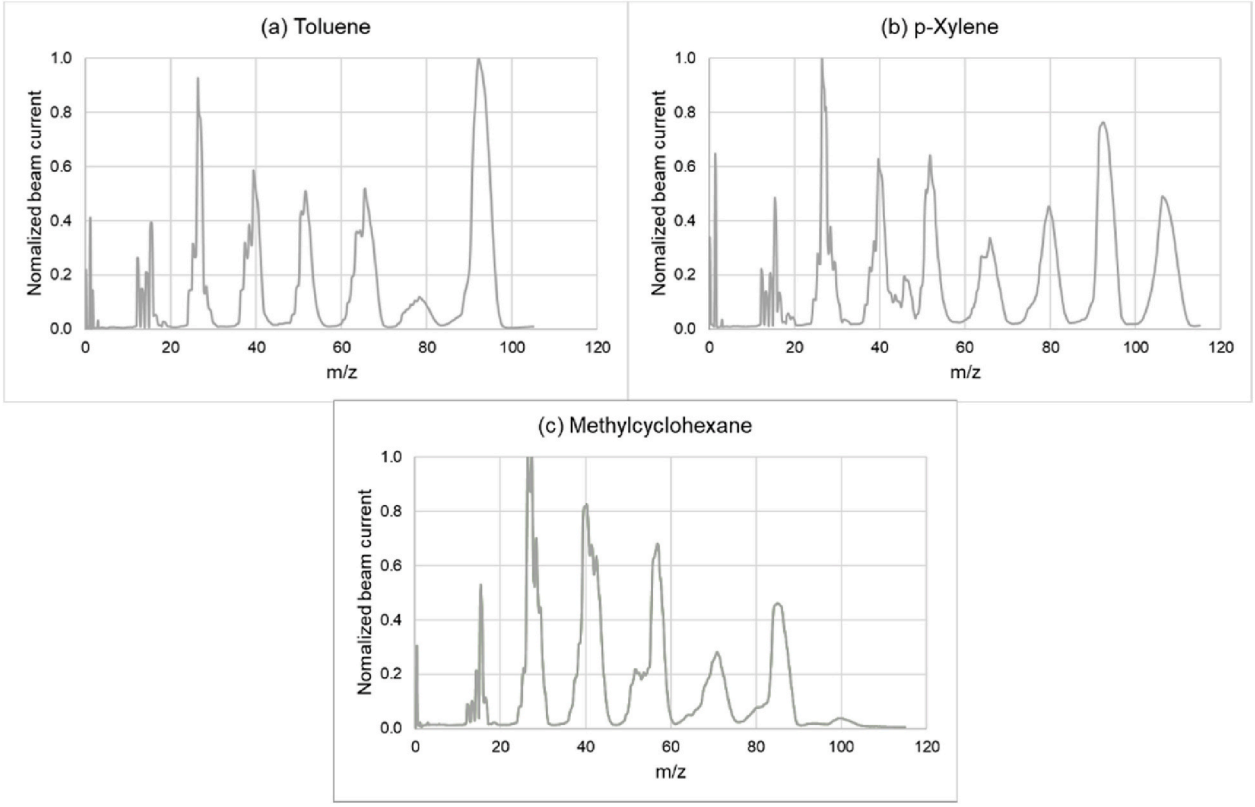

Fig. 3. Molecular carbon actual mass spectrum, (a) Toluene (C_7H_8), (b) p-Xylene (C_8H_{10}), (c) Methylcyclohexane (C_7H_{14}) with mass resolution M/dM of 35.

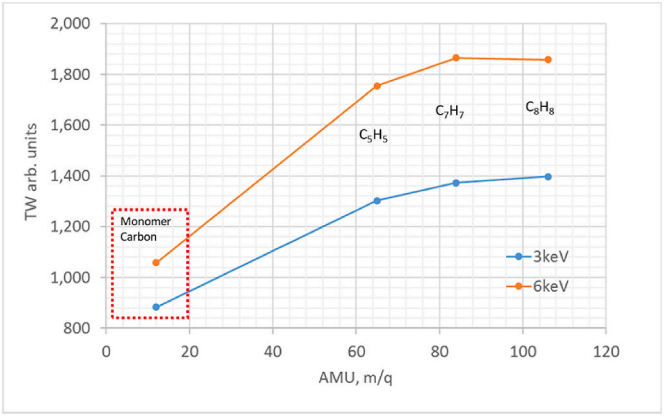

Fig. 4. Implant damage comparison according to mass increase for mid - E^{14}/cm^2 implantation by using KLA TP630™.

Our goal in this work is to implant carbon beams into silicon. The carbon that is implanted can either be a monomer (C^+) or a molecular (C_x^+) species; the atomic weight of the implanted species will alter the damage profile of the implant. A typical electron fragmentation interaction would be, for toluene (C_7H_8) in example:

$$C_7H_8 + e^- \rightarrow (CH)_x^+ + 2e^-$$

with x = 2–8, the molecular fragments.

Choosing the proper precursor to achieve the desired profile is important. There are many kinds of carbon compounds in nature [13]. As mentioned above, the precursor should be compatible with ion source gas delivery and extraction, and require no additional hardware for incorporation into a standard ion implanter [18].

In addition, we want to use higher mass for this test. Mass spectrum (electron ionization) reference data are available on many candidate materials, and was used to find suitable materials; examples are shown in Fig. 2.

In this study, we performed two different carbon energy implants, 3 keV and 6 keV with n-type doped <100> silicon wafer. The conditions were simulated based on recent shallow junction doses and energies used in memory devices. Implants at mid-E^{14}/cm^2 dose were completed for each various carbon content species: (C_1), C_5 H_5, C_7 H_7, and C_8H_8. The ion implanter has a magnet capable of filtering each species, so the exact AMU being implanted is known. The effective energies were derived from the known moiety being implanted and referenced to the monomer C^+. (For instance, $C_7H_7^+$ extracted at 22.75 keV gives an energy equivalence of 3 keV monomer carbon). We measured all samples with ThemaWave™ (TW) to compare implant damage. The ThermaWave™ is an optical measurement technique that reports change in reflectance as the system is thermally pumped with a laser [19]. The response, TW units, is proportional to implant damage, with higher TW values indicating more damage. In the context of this work, implant damage is an indication of displaced Si atoms from their original lattice positions, up to the formation of an amorphous layer. Implant damage is well studied and has been reported in detail [20]. Moreover, we measured monomer and molecular samples by using Transmission Electron Microscopy (TEM) to compare amorphization layer thickness.

3. Results and discussion

Based on previous work on electron fragmentation of aromatic hydrocarbon species, we performed mass spectrum of each candidate material, Toluene (C_7H_8), p-Xylene (C_8H_{10}), and Methyl cyclohexane (C_7H_{14}) with HCP source in Fig. 3. The AMU spectrum indicate a different distribution of carbon species than those obtained in Fig. 2. This phenomenon may be due to a cracking pattern (fragmentation) that depends on plasma operating conditions, including, for instance plasma arc or cathode power control [17]. Toluene has larger variations in beam current depending on the mass (C_3, C_5, C_7). Methylcyclohexane has low beam current at the higher mass range which is most common application so was ranked lower priority. We selected p-Xylene for this work because it has a broad mass spectrum (C_3, C_5, C_6, C_7, and C_8) with reasonable beam current. The other molecules could be used theoretically but the p-xylene score highest for the desired effects.

Larger molecular weight species give higher TW values, as observed in Fig. 4. For the 3 keV case, the ThermaWave™ value increases as implanted mass increases, as expected. In 6 keV case, C_7H_7 and C_8H_8 value are close to each other, which means implant damage saturates as mass increases. This condition typically signifies a fully developed

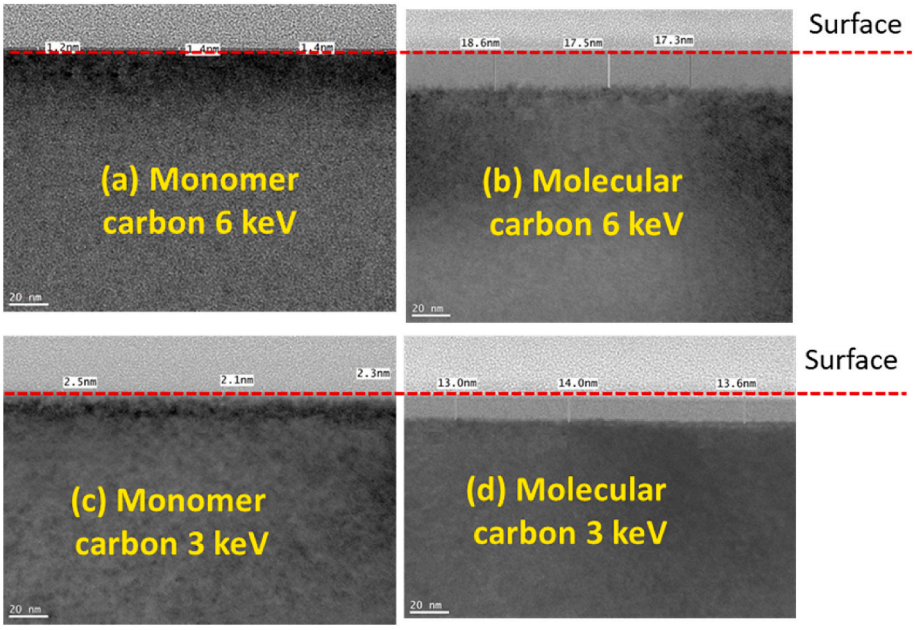

Fig. 5. Cross-section TEM analysis results, (a) 6 keV monomer carbon, (b) 6 keV molecular carbon with C_7H_7+, (c) 3 keV monomer carbon, (d) 3 keV molecular carbon with C_7H_7+.

amorphous layer that will not change with increasing dose of implant.

We used TEM analysis method to compare amorphization layer between monomer carbon and molecular carbon (C_7H_7+) in Fig. 5 [21]. We could not observe amorphization layer on 3 keV and 6 keV monomer carbon. On the other hand, 6 keV Molecular carbon showed 17.3–18.6 nm amorphization layer and 3 keV Molecular carbon has 13.0–14.0 nm. The lack of distinct structures, including micro-crystalline pockets, means the layer has been fully amorphized.

As a result, we could find the proper material from Aromatic Hydrocarbon for molecular carbon implant by using HCP on existing system without additional complex or complicated source technologies.

4. Conclusions

Carbon implant is widely used for suppressing Boron TED effect [5]. In addition to carbon implant, additional PAI process is required on Ultra Shallow Junction (USJ) [8]. In this study, we found a proper material using aromatic hydrocarbons for molecular carbon implant without vaporizer by using HCP on existing system. We expect the improved device characteristic and performance with self-amorphization layer by using molecular carbon implantation. The potential molecular carbon applications are co-implant for Ultra Shallow Junction (USJ) & halo as well as contact resistivity reduction [22].

Credit author statement

KyungWon Lee: Conceptualization, Methodology, Writing - Original Draft, Visualization.

Michael Saied Ameen: Conceptualization, Methodology, Investigation, Writing - Review & Editing.

Mark Alan Harris: Methodology, Writing - Review & Editing.

Dwight Dongwan Roh: Formal analysis, Validation.

Ronald Norman Reece: Resources, Visualization, Project administration.

DaeHo Yoon: Validation, Writing - Review & Editing, Supervision.

All authors contributed to writing this manuscript.

Declaration of competing interest

The authors declare that they have no known competing financial interests or personal relationships that could have appeared to influence the work reported in this paper.

Acknowledgments

The authors would like to thank the technical team of Axcelis Technologies, Inc. ATC (Advanced Technology Center) to evaluate characteristic of the molecular carbon.

References

[1] Robert H. Dennard, et al., Design of ion-implanted MOSFET's with very small physical dimensions, IEEE J. Solid State Circ. 9 (5) (1974) 256–268.
[2] S.M. Sze, K.K. Ng, Physics of Semiconductor Devices, John Wiley & Sons, New York, NY, USA, 2006.
[3] P.A. Stolk, et al., Physical mechanisms of transient enhanced dopant diffusion in ion-implanted silicon, J. Appl. Phys. 81 (9) (1997) 6031–6050.
[4] T.O. Sedgwick, et al., Transient boron diffusion in ion-implanted crystalline and amorphous silicon, J. Appl. Phys. 63 (5) (1988) 1452–1463.
[5] P.A. Stolk, et al., Carbon incorporation in silicon for suppressing interstitial-enhanced boron diffusion, Appl. Phys. Lett. 66 (11) (1995) 1370–1372.
[6] Seong-Dong Kim, et al., Advanced source/drain engineering for box-shaped ultrashallow junction formation using laser annealing and pre-amorphization implantation in sub-100-nm SOI CMOS, IEEE Trans. Electron. Dev. 49 (10) (2002) 1748–1754.
[7] Park, Bo Hyun. 1998, Method for Forming Shallow Junction for Semiconductor Device. Hyundai Electronics Industries C., Ltd., Kyoungki-do, U.S. Patent No. vol. 5,795,808.
[8] Schreutelkamp, et al., Pre-amorphization damage in ion-implanted silicon, Mater. Sci. Rep. 6 (7-8) (1991) 275–366.
[9] Gibbons, et al., Ion implantation in semiconductors—Part II: damage production and annealing, Proc. IEEE 60 (9) (1972) 1062–1096.
[10] Dearnaley, et al., Ion implantation in semiconductors, Phys. Bull. 20 (5) (1969) 165.
[11] F.F. Morehead, et al., Formation of amorphous silicon by ion bombardment as a function of ion, temperature, and dose, J. Appl. Phys. 43 (3) (1972) 1112–1118.
[12] Michael Nastasi, et al., Ion implantation in CMOS Technology: machine challenges, in: Ion Implantation and Synthesis of Materials, Springer, Berlin, Heidelberg, 2006.
[13] Jacobson, et al. 2011, Cluster Ion Implantation for Defect Engineering. SEMEQUIP, Inc., Massachusetts U.S. Patent No. vol. 7,919,402.
[14] Karuppanan Sekar, et al., Cluster carbon implants—cluster size and implant temperature effect, in: 11th International Workshop on Junction Technology (IWJT), IEEE, 2011.
[15] Karuppanan Sekar, et al., Annealing behavior of clustercarbon™ implants, in: 16th IEEE International Conference on Advanced Thermal Processing of Semiconductors, IEEE, 2008.
[16] N. Angert, Ion sources, CAS CERN Accel. Sch.: 5 General Accl. Phys. Course Vol 2 Proc. (1994) 537.
[17] Ian G. Brown, The Physics and Technology of Ion Sources, John Wiley & Sons, 2004.
[18] Linstrom, P. J., and W. G. Mallard. "NIST Chemistry Webbook (http://webbook.nist.Gov/chemistry)." NIST Standard Reference Database 69.
[19] D.E. Kamenita, R.B. Simonton, Sources of variation in Therma Wave measurements of ion implanted wafers, Nucl. Instrum. Methods B74 (1993) 234–237.
[20] Schreutelkamp, et al., Pre-amorphization damage in ion-implanted silicon, Mater. Sci. Rep. 6 (7-8) (1991) 275–366.
[21] S. Prussin, et al., Formation of amorphous layers by ion implantation, J. Appl. Phys. 57 (2) (1985) 180–185.
[22] Pankaj Kalra, Advanced Source/Drain Technologies for Nanoscale CMOS, University of California, Berkeley, 2008.